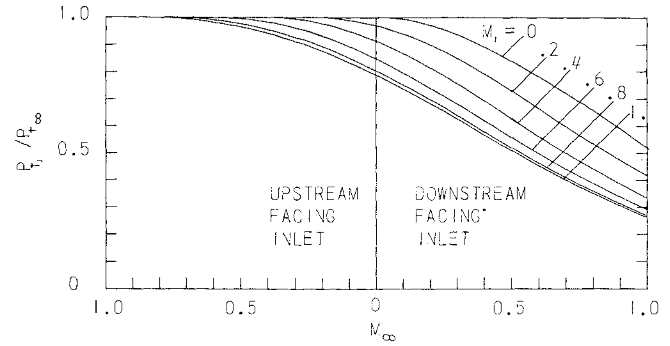

Fig. 1 Total pressure recovery vs freestream mach number for various inlet mach numbers.

$$(A_1/A_\infty) = (M_\infty/M_1)(P_\infty/P_1)\left(\frac{T_1}{T_\infty}\right)^{1/2} \quad (1)$$

$$\Phi_1 + \Phi_\infty = 0 \quad (2)$$

where A is the area, M the Mach number, P the static pressure, T the static temperature, and Φ the momentum parameter equal to: $[(P - P_\infty) + \gamma PM^2]\,A$. Also, subscript 1 refers to a location within the inlet where the flow is uniform and subscript ∞ denotes an external uniform flow location far upstream of the inlet. It should be mentioned that Eq. (2) is based on the assumption that intake lip is sharp and therefore cannot support a suction force and that the pressure integral over the control surface vanishes for reasons detailed in Ref. 1.

When the area ratio is eliminated between Eqs. (1) and (2), and use is made of the stagnation property relations for temperature and pressure, we obtain

$$\frac{P_{t1}}{P_{t\infty}} = \frac{\left(\dfrac{1 + \frac{\gamma-1}{2}M_1^2}{1 + \frac{\gamma-1}{2}M_\infty^2}\right)^{\frac{\gamma+1}{2(\gamma-1)}}}{(1 + \gamma M_1^2)\left(\dfrac{1 + \frac{\gamma-1}{2}M_\infty^2}{1 + \frac{\gamma-1}{2}M_1^2}\right)^{1/2} + \gamma M_1 M_\infty} \quad (3)$$

Thus the total pressure recovery, $P_{t(1)}/P_{t\infty}$, is a function of just the freestream and duct Mach numbers. In addition, it can be seen that the direction of the freestream flow affects the magnitude of the recovery only through the $\gamma M_1 M_\infty$ term. Figure 1 is the graph of the expression. Notice that pressure recoveries found from values of M_∞ to the right of the origin correspond to an upstream facing intake. Total pressure ratios are much lower in the downstream facing duct case. Furthermore, the maximum total pressure, for a given duct Mach number, that can be recovered with a rear facing sharp-lip inlet occurs as the freestream Mach number approaches zero. When $M_\infty = 0$, (static case), the total pressure recovered equals the freestream static pressure, P_∞. Thus at best, there is a complete loss of the freestream dynamic head.

Finally, it should be pointed out that type of inlet considered in this note produces a larger total pressure loss than would occur in a variable area or flared inlet, which is a physically more realistic intake. On the other hand, a well rounded inlet, which is clearly not a practical exhaust nozzle when the propulsion unit is used to develop forward thrust, is capable of complete total pressure recovery. Thus the actual intake experiences total pressure losses somewhere between those predicted here and unity. However, since reverse thrust applications occur at low Mach numbers and therefore at the largest values of pressure recovery, these differences should not be unreasonable.

References

[1]Fradenburg, E. A. and Wyatt, D. D., "Theoretical Performance Characteristics of Sharp-Lip Inlets," TN 3004, 1953 NACA.

Cavity Growth and Collapse Phase of Hydraulic Ram

G. C. Cardea* and P. J. Torvik†

Air Force Institute of Technology, Wright-Patterson Air Force Base, Ohio

Introduction

WHEN a projectile traveling at a high rate of speed encounters a liquid-filled container, several mechanisms contribute to the generation of high pressures within the liquid. The generation of these large pressures is referred to as the hydraulic ram phenomenon.[1] Such high pressures may cause the growth of cracks emanating from the entrance or exit hole and lead to rupture of a tank wall. High internal pressures also may cause bulging of tank walls and damage to the supporting structure. Finally, any equipment inside the container may be damaged by high pressure.

Several mechanisms can lead to the generation of pressures large enough to produce damage. As the projectile strikes and penetrates the entrance wall, a strong shock wave will be driven into the fluid. This phenomenon has been the subject of a number of studies.[2,3] As the projectile moves through the fluid, a pressure field in generated around the projectile. This phase of the process, which is made quite complex by the tumbling which typically occurs when projectiles pass through liquids, has been considered quite extensively.[1] The third phase, the subject of the present study, is the generation of pressures due to the formation and collapse of the cavity which forms behind the projectile. It has been noted previously that such cavities will form, will generate pressures, and are loosely analogous to cavities formed by underwater explosions.[1]

It is the purpose of this note to show that the formulae developed for the purpose of analyzing underwater explosions can be adapted to projectile penetration and used to predict the relationships between the period of the cavity growth and collapse cycle, the energy required to produce the cavity, the maximum size of the cavity, and the peak pressures generated by its collapse. Some experimental data are used to confirm the applicability of such predictions.

Received January 15, 1974. Based on a thesis submitted in partial fulfillment of the requirements for the Master of Science degree. We are indebted to C. C. Gebhard of the Air Force Flight Dynamics Laboratory for allowing us to use his unpublished experimental data.

Index categories: Aircraft Fuels and Fuel Systems; Aircraft Structural Design (Including Loads); Military Aircraft Missions.

*Presently Flight Test Engineer, Edwards Air Force Base, Calif.

†Professor of Mechanics.

Analysis

Cavitation begins almost immediately after a liquid-filled container is penetrated by a projectile traveling at ballistic speeds. Examination of high-speed motion pictures of bullets passing through water-filled tanks revealed that the cavity begins as a small nearly cylindrical wake which grows markedly after tumbling occurs and remains in the liquid after the projectile has passed through. The cavity increases in size to a maximum radius at which time it is approximately spherical and then collapses to a minimum radius. This process of growth and collapse is repeated several times (cavity oscillation). Each time a minimum radius occurs (cavity collapse), a pressure pulse is propagated into the fluid and the cavity expands once again (cavity rebound). Due to losses in the fluid, each succeeding cycle of the oscillation leads to a smaller cavity, a lower-peak pressure, and a reduced period. In a finite tank, reflections of the succession pulses from the walls will further complicate the pressure history at any point.

The same sequence of events results from the underwater detonation of an explosive. If the explosion occurs at a depth sufficient to insure that there is no surface interference, a bubble of gaseous products expands radially against the ambient pressure in the fluid and creates a spherical bubble. The amount of energy required to create a cavity of radius a_m in an incompressible fluid at ambient pressure P_o is the product of the pressure and the change in volume of the body of fluid containing the cavity.

$$E_c = 4\pi a_m{}^3 P_o/3 \tag{1}$$

The second result which we will adapt from the theory of underwater explosions is the Willis formula,[4] an expression for the time required for the bubble to expand to the maximum radius and collapse to a minimum, i.e., the period of cavity oscillation. If the maximum radius is assumed large in comparison to the minimum radius, the period is

$$T = 1.14\rho_o{}^{1/2}E_c{}^{1/3}/P_o{}^{5/6} \tag{2}$$

where T is the cavity period and ρ_o is the density of the medium. The third necessary relationship is that between the energy in the explosion and the peak pressure occurring at a distance R from the cavity center. This equation has been used[4] to predict the relationship between the weight of TNT detonated and the magnitude of the pressure field around the bubble at the time of its first minimum (the secondary pulse).

$$P_{max} - P_o = 2590W^{1/3}/R \tag{3}$$

In the above, $P_{max} - P_o$ is the gage pressure in psi, W is the weight of detonated TNT in pounds, and R is the distance from the center of the cavity in feet. In predicting the effects of underwater explosions,[4] it is assumed customarily that only 50% of the energy content of the explosive goes into the creation of the cavity. If the driving energy, period of oscillation, peak pressure at some R, or the maximum cavity size is known, Eqs. (1–3) may be used to compute the other three. The cavity period is the easiest to measure experimentally as it is not subject to the uncertainties of pressure gage calibration or the location of the cavity center. Assuming that only 50% of the energy contained in a pound of TNT (1.514×10^6 ft-lb) is converted into cavity energy, Eq. (3) can be rewritten as

$$P_{max} - P_o = 28.5E_c{}^{1/3}/R \text{ psi}(\text{ft}^{2/3}/\text{lb}^{1/3}) \tag{4}$$

where E_c is as previously defined.

Table 1
Computed and observed cavity parameters

Shot no.	V fps	Observed T msec	R ft	R ft	Computed E_c, ft-lb	$R(P_{max} - P_o)$ ft-psi
2	1269	24.8	0.5	0.494	876	272
3	1209	26.2	0.5	0.522	1032	288
4	1254	26.9	0.5	0.536	1117	295
5	1215	26.9	0.5	0.536	1117	295

Verification

The predictions were compared to the results of a previously conducted series of experiments in which 0.50 in. caliber projectiles were fired into cubical containers (three-foot sides) of water containing four-pressure transducers. Time histories of the pressure readings at each of the four transducers were made, and the cavity resulting from each shot was documented by high-speed motion pictures taken through a transparent tank wall. Using a density of 1.94 slugs/ft^3, an ambient pressure of 2210 lbs per ft^2, and the measured cavity period, maximum cavity radii and cavity energies were computed using Eqs. (1) and (2) and are given in Table I. Results given are for four shots, nominally identical. The observed maximum cavity radius was determined to be about 0.5 ft ± 10% for each of the shots which, considering the uncertainty resulting from determining cavity size from a motion picture record, is considered to be in agreement with the computed values.

The predicted energies also appear to be reasonable as can be seen from consideration of the drag, i.e., the energy deposited per unit length of projectile travel, which is

$$E' = D = C_D\rho_o V^2 S/2 \tag{5}$$

where S is the cross-sectional area of the projectile, C_D is the drag coefficient, ρ_o the density of the fluid, and V the velocity of the projectile. The drag coefficient for an untumbling projectile in fully cavitating flow[5] is 0.3. For a fully tumbling projectile, C_D has been estimated[1] to be about 1.67. At the average velocity for these four shots the energy deposited in one foot of travel is 540 ft-lb and 1845 ft-lb for the two values of C_D, respectively. These numbers are observed to bound the amount of energy calculated as being required to generate cavities of the observed size, one foot in diameter. If 540 ft-lb are lost in the first foot of travel and tumbling is then assumed to occur, the energy deposited in the second foot is 1450 ft-lb. Since not all the energy deposited need go into the radial velocity field of an expanding cavity, it is to be expected that the available energy (the drag) is greater than that required to form the cavity.

A comparison of the calculated and observed pressures is more difficult, for the peak overpressure recorded depends on the distance from the gage to the cavity center. The motion picture records of the experiments did not provide a determination of the distance from cavity center to pressure transducer accurate enough to permit a comparison of observed and calculated products of pressure and distance. However, from the predicted value of the product of pressure and distance for each shot and from the recorded value of peak pressure at each gage, a locus of possible cavity centers was constructed for each gage and their intersection determined. In all cases this computed location of the cavity center was found to be in reasonable agreement with what could be observed from the motion pictures, confirming that pressures at any point may be predicted if the location of the cavity center is known. These results are not entirely conclusive, as not all gages were operative in all of the shots. It can be seen from the table that pressures of considerable significance (several hundred psi) occur a foot away from the cavity center.

References

[1]Lundstrom, Eric A. *Fluid Dynamic Analysis of Hydraulic Ram*, NWC Technical Publication 5227, July 1971, Naval Weapons Center, China Lake, Calif.

[2]Torvik, P. J. and Clark, J. W. "The Reduction of Impact Induced Pressures in Fuel Tanks," *43rd Shock and Vibration Bulletin*, Pt. 2, June 1973, pp. 203–208.

[3]Ball, R. E., Power, H. L., and Fuhs, A. E. "Fuel Tank Wall Response to Hydraulic Ram during the Shock Phase," *Journal of Aircraft, Vol. 10*, No. 9, Sept. 1973, pp. 571–572.

[4]Cole, R. H. *Underwater Explosions*, Princeton University Press, Princeton, N.J., 1948, pp. 275, 276, 364.

[5]Hoerner, S. F. *Fluid Dynamic Drag*, Hoerner, Midland Park, N.J., 1958.

Computation of Transonic Flow about Lifting Wing-Cylinder Combinations

E. B. Klunker* and P. A. Newman*

NASA Langley Research Center, Hampton, Va.

SUCCESSFUL development of relaxation algorithms for the computation of inviscid potential flow about two-dimensional airfoils and bodies of revolution at transonic speeds[1-8] has led to adaptation of the technique to more complex configurations. Three-dimensional wing calculations based upon a small disturbance potential equation have been presented in Refs. 9–13 and calculations for a yawed wing with the full potential equation are described in Ref. 14. To date, the only published results for a wing-body configuration are for a nonlifting wing with a cylindrical body.[12] Some results are presented here for a lifting rectangular wing centrally located on a circular-cylindrical body. This simple configuration has been utilized in order to assess the merits of a mapping technique for wing-body configurations.

Two general approaches can be followed in the formulation of these problems: 1) employ Cartesian (or other simple) coordinates which preserve the utmost simplicity in the governing differential equation but which generally necessitate interpolation or extrapolation to incorporate some of the boundary conditions, or 2) utilize coordinate transformations which simplify specification of the surface boundary conditions but which generally increase the complexity of the differential equation. The first technique has been used in Ref. 15 for a two-dimensional time-dependent computation while the second has been widely employed in fluid mechanics and other fields. A combination of the two approaches will most likely be required for all but the simplest configurations. The procedure employed here makes use of a coordinate transformation to simplify specification of the surface boundary condition in the computation of the flow about a rectangular wing symmetrically located on a circular-cylindrical body. The method can be extended to incorporate wing sweep, finite length body of noncircular cross section, and arbitrary wing placement; however, these extensions involve a considerable increase in complexity of the problem.

Received January 18, 1974.

Index categories:

* Aerospace Technologists, High-Speed Aircraft Division.

Method

One of the simplest wing-body configurations which can be reduced to a simple form by a coordinate transformation is that of a cylindrical body with the wing plane passing through the body axis. A Joukowski-type transformation in planes normal to the body axis

$$\sigma = \sigma_1 + c^2/\sigma_1 \quad x = x_1 \quad \sigma_1 = y_1 + iz_1 \quad \sigma = y + iz \qquad (1)$$

where c is a constant, maps the circular cross section $y_c^2 + z_c^2 = c^2$ ($y = y_c$, $z = z_c$ on c) and the plane $z = 0$ for $|y| \geq c$ onto the plane $z_1 = 0$. If the body radius does not differ appreciably from c, then the boundary condition of zero normal velocity both on the wing and on the body can be enforced on the plane $z_1 = 0$. Moreover, the boundary condition on the trailing vortex sheet, which is assumed to lie in the plane of the wing, is similarly satisfied on the plane $z_1 = 0$. The condition that c is a constant preserves the orthogonality of the coordinates but excludes consideration of bodies of finite length. The body radius r_o can depend both on x and the polar angle $\Theta = \arctan(z_o/y_o)$; however, one-to-one correspondence between the coordinate systems x,y,z and x_1,y_1,z_1 requires that $r_o \geq c$. Thus the boundary-value problem for this simple wing-body configuration in the x_1,y_1,z_1 coordinates is similar in most respects to that of a wing alone in Cartesian coordinates.

The equation for the pertubation velocity potential used here is

$$[\beta^2 - (\gamma + 1)M_\infty{}^2\phi_x(1 + \phi_x/2)]\phi_{xx} + \phi_{yy} + \phi_{zz} = 0 \qquad (2)$$

where M_∞ is the stream Mach number, $\beta^2 = 1 - M_\infty{}^2$, and γ is the ratio of specific heats. Equation (2) differs from the familiar form of the small disturbance transonic flow equation by inclusion of the term $\phi_x{}^2\phi_{xx}$ which has been retained to better approximate the critical speed where the equation changes type from elliptic to hyperbolic.

The flow tangency condition on the wing is approximated by

$$\phi_z(x, y, 0) = f_x - \alpha \qquad (3)$$

for x,y on the wing planform where $z = f(x,y)$ is the equation of the wing surface and α is the angle of incidence. It may be noted here that taking the surface boundary condition as $\phi_z(x,y,0) = [1 + \phi_x(x,y,0)]f_x - \alpha$ generally leads to results where the full expansion around the blunt leading edge of an airfoil is not achieved. The flow tangency condition for a body of revolution is approximated by

$$y_c\phi_y(x, y_c, z_c) + z_c[\alpha + \phi_z(x, y_c, z_c)] = c(dr_0/dx) \qquad (4)$$

Additional terms involving $(dr_o/d\theta)$ must be included in Eq. (4) for bodies of noncircular cross section. The boundary condition on the trailing vortex sheet, assumed to lie in the plane of the wing $z = 0$, is

$$\phi(x, y, 0^+) - \phi(x, y, 0^-) = \Gamma(y) \qquad (5)$$

for x,y on the sheet; the circulation $\Gamma(y)$ is determined as part of the solution.

The disturbance velocity potential must vanish far from the wing-body configuration and its trailing vortex sheet. Thus, $\phi = 0$ on the outer boundary surfaces except those far upstream and far downstream in the vicinity of the